8-6-2019

What Is the Accuracy Limit of Adiabatic Linear-Response TDDFT Using Exact Exchange–Correlation Potentials and Approximate Kernels?

Jaspreet Kaur

Egor Ospadov

Viktor N. Staroverov

What is the Accuracy Limit of Adiabatic Linear-Response TDDFT Using Exact Exchange-Correlation Potentials and Approximate Kernels?

Jaspreet Kaur, Egor Ospadov, and Viktor N. Staroverov*

Department of Chemistry, The University of Western Ontario, London, Ontario N6A 5B7, Canada

(Dated: August 5, 2019)

Abstract

Calculation of vertical excitation energies by the adiabatic linear-response time-dependent density-functional theory (TDDFT) requires static Kohn–Sham potentials and exchange-correlation kernels. When these quantities are derived from standard density functionals, mean absolute errors (MAE) of the method are known to range from 0.2 eV to over 1 eV, depending on the functional and type of excitation. We investigate how the performance of TDDFT varies when increasingly accurate exchange-correlation potentials derived from Hartree–Fock (HF) and post-HF wavefunctions are combined with different approximate kernels. The lowest MAEs obtained in this manner for valence excitations are about 0.15–0.2 eV, which appears to be the practical limit of the accuracy of TDDFT that can be achieved by improving Kohn–Sham potentials alone. These findings are consistent with previous reports on the benefits of accurate exchange-correlation potentials in TDDFT, but provide new insights and afford more definitive conclusions.

Corresponding Author

*E-mail: vstarove@uwo.ca

ORCID: 0000-0002-6828-3815

1. BACKGROUND

The linear-response time-dependent density-functional theory[1–3] (TDDFT) is a widely used method for calculating excitation energies of many-electron systems. The central role in this technique is played by the interacting density-response function

$$\chi[\rho_0](\mathbf{r},\mathbf{r}',t-t') = \left.\frac{\delta\rho(\mathbf{r},t)}{\delta v_{\mathrm{ext}}(\mathbf{r}',t')}\right|_{\rho=\rho_0}, \tag{1}$$

which describes the linear part of the response of the ground-state density $\rho_0(\mathbf{r},t)$ to a weak perturbation of the external potential $v_{\mathrm{ext}}(\mathbf{r}',t')$. The key idea of the linear-response method is to extract excitation frequencies of the system as poles of the density-response function Fourier-transformed to the frequency domain, $\chi(\mathbf{r},\mathbf{r}',\omega)$. One way to see what this requires is to represent $\chi(\mathbf{r},\mathbf{r}',\omega)$ by a Dyson-type equation[4]

$$\begin{aligned}\chi(\mathbf{r},\mathbf{r}',\omega) = \chi_s(\mathbf{r},\mathbf{r}',\omega) + \int d\mathbf{r}_1 \int d\mathbf{r}_2\, \chi_s(\mathbf{r},\mathbf{r}_1,\omega) \\ \times \left[\frac{1}{|\mathbf{r}_1-\mathbf{r}_2|} + f_{\mathrm{XC}}(\mathbf{r}_1,\mathbf{r}_2,\omega)\right] \chi(\mathbf{r}_2,\mathbf{r}',\omega),\end{aligned} \tag{2}$$

where $\chi_s(\mathbf{r},\mathbf{r}',\omega)$ is the noninteracting density response function expressible in terms of the unperturbed Kohn–Sham orbitals and orbital energies, while $f_{\mathrm{XC}}(\mathbf{r},\mathbf{r}',\omega)$ is the Fourier transform of the exchange-correlation kernel,

$$f_{\mathrm{XC}}[\rho_0](\mathbf{r},\mathbf{r}',t-t') = \left.\frac{\delta v_{\mathrm{XC}}(\mathbf{r},t)}{\delta\rho(\mathbf{r}',t')}\right|_{\rho=\rho_0}, \tag{3}$$

where $v_{\mathrm{XC}}(\mathbf{r},t)$ is the exchange-correlation potential. Thus, the two quantities needed to set up eq 2, $\chi_s(\mathbf{r},\mathbf{r}',\omega)$ and $f_{\mathrm{XC}}(\mathbf{r},\mathbf{r}',\omega)$, are determined by $v_{\mathrm{XC}}(\mathbf{r},t)$. To extract the poles of $\chi(\mathbf{r},\mathbf{r}',\omega)$, this function is usually expanded in products of occupied and virtual Kohn–Sham orbitals and eq 2 is cast as a matrix eigenvalue problem known as Casida's equations.[5] Solution of Casida's equations produces excitation energies and expansion coefficients of $\chi(\mathbf{r},\mathbf{r}',\omega)$.

In principle, the linear-response TDDFT is exact, but to take full advantage of this promise one needs the exact Kohn–Sham orbitals and orbital eigenvalues as well as the exact $f_{\mathrm{XC}}(\mathbf{r},\mathbf{r}',\omega)$. The exact Kohn–Sham orbitals are already challenging to obtain, and the exact frequency-dependent kernel is even less accessible. To make progress, the problem is simplified by introducing the adiabatic approximation

$$v_{\mathrm{XC}}[\rho](\mathbf{r},t) = \left.\frac{\delta E_{\mathrm{XC}}[\rho]}{\delta\rho(\mathbf{r})}\right|_{\rho=\rho_t}, \tag{4}$$

where $E_{\mathrm{XC}}[\rho]$ is the ground-state exchange-correlation energy functional. Under this assumption, the exchange-correlation kernel becomes frequency-independent and the quantities required to set up Casida's equations are just the static exchange-correlation potential,

$$v_{\mathrm{XC}}[\rho](\mathbf{r}) = \frac{\delta E_{\mathrm{XC}}[\rho]}{\delta \rho(\mathbf{r})}, \tag{5}$$

and its functional derivative,

$$f_{\mathrm{XC}}[\rho](\mathbf{r}, \mathbf{r}') = \frac{\delta v_{\mathrm{XC}}[\rho](\mathbf{r})}{\delta \rho(\mathbf{r}')} = \frac{\delta^2 E_{\mathrm{XC}}[\rho]}{\delta \rho(\mathbf{r}) \delta \rho(\mathbf{r}')}, \tag{6}$$

both evaluated at $\rho_0(\mathbf{r})$. The adiabatic approximation makes it possible to use the linear-response TDDFT machinery with a wide range of approximate ground-state exchange-correlation functionals available in quantum-chemistry packages.[6–9] It is worth noting that the adiabatic form of Casida's equations can also be derived without the response-function formalism by using only the variational principle.[10]

The adiabatic approximation itself is remarkably accurate,[1] at least for single excitations,[11] but the errors caused by the use of approximate $v_{\mathrm{XC}}(\mathbf{r})$ and $f_{\mathrm{XC}}(\mathbf{r}, \mathbf{r}')$ are substantial, typically 0.2–0.5 eV for valence and up to 1 eV or more for Rydberg excitations, depending on the functional.[12–22] The errors in ground-state exchange-correlation potentials were initially believed to be dominant, as they demonstrably are for Rydberg transitions,[23–28] but the errors in static kernels can also be significant.[1,29] Because exchange-correlation potentials are simpler and more familiar objects than the kernels, there have been several attempts to improve the performance of adiabatic TDDFT by replacing standard density-functional approximations for $v_{\mathrm{XC}}(\mathbf{r})$ with model[23,24,29–31] and optimized effective potentials[32–35] (OEPs). Because the kernels corresponding to OEPs and most model potentials must themselves be evaluated by indirect methods,[35–37] accurate Kohn–Sham potentials in practice are often paired with static kernels derived from standard density functionals such as the local density approximation (LDA).

2. PROBLEM STATEMENT

Given that accurate Kohn–Sham effective potentials can be constructed with less effort than accurate exchange-correlation kernels, it is natural to wonder how far one can increase the accuracy of adiabatic TDDFT by improving the potentials alone. Evidence based on

model potentials[31,38,39] is encouraging but inconclusive because model potentials are not particularly accurate.[40] Most TDDFT studies that did employ accurate Kohn–Sham potentials were restricted to two-electron systems,[32,33] small atoms,[41] LDA kernel,[34,41] or the exchange-only case.[37] A study by Allen and Tozer[42] went beyond these limits, but was modest in scope (13 selected excitation energies of N_2 and CO using two different kernels). The most extensive assessment of nearly exact Kohn–Sham orbitals and orbital energies in TDDFT was reported recently by Jin *et al.*,[43] but their work dealt with a variant of the random-phase approximation in which $f_{\mathrm{XC}}(\mathbf{r}, \mathbf{r}')$ is ignored entirely.

In this work, we assess the benefit of exact Kohn–Sham potentials in adiabatic TDDFT using our recently developed method for constructing accurate exchange[44,45] and exchange-correlation[46–48] potentials from *ab initio* wavefunctions. Two specific questions are posed here: (1) How far can one push the accuracy of adiabatic TDDFT by using accurate Kohn–Sham potentials and standard (local, semilocal, and hybrid) approximations for exchange-correlation kernels? (2) Which approximate kernels work best with accurate exchange-correlation potentials? These questions were anticipated but not specifically addressed in existing literature.[32–34,41,42] To focus on just one problem, we limit the scope of this work to excitations without charge-transfer character.

3. METHODOLOGY

An adiabatic linear-response TDDFT calculation involves two steps. First, one solves the Kohn–Sham equations to generate ground-state Kohn–Sham orbitals and orbital energies. In the second step, those quantities are used to set up and solve Casida's eigenvalue equations. The Kohn–Sham orbitals and their energies were obtained from various density-functional approximations (see below) and from all-electron *ab initio* wavefunctions using our recently developed method[46–48] implemented locally in the *Gaussian* program[49] as described in ref 48. The wavefunctions were Hartree–Fock (HF) and complete active space (CAS) self-consistent field (SCF).

The static exchange-correlation kernels were computed at the four rungs of Jacob's ladder:[50,51] LDA in the Perdew–Wang parametrization for the correlation energy,[52] the Perdew–Burke–Ernzerhof (PBE) generalized gradient approximation (GGA),[53] the revised Tao–Perdew–Staroverov–Scuseria (rTPSS) meta-GGA,[54] and the PBE0 hybrid

functional.[55,56] All of these kernels were constructed in a post-SCF manner from the Kohn–Sham orbitals generated in the first step. Full exchange-correlation kernels were used even for Kohn–Sham potentials derived from HF (exchange-only) wavefunctions.

Our methodology constrains us to use the same one-electron basis set for computing all quantities and properties from wavefunctions to excitation energies. The latter property restricts our choices to basis sets with sufficiently diffuse functions. We selected three such basis sets: for atoms—the universal Gaussian basis set (UGBS) augmented with polarization and diffuse functions (see below); for small molecules—Sadlej+,[38,57] taken the Basis Set Exchange database;[58] for larger molecules—6-311++G(3df,3pd).

The test sets of excitation energies and experimental reference data for our assessment were those used by Savin *et al.*[59] (Be atom), Tozer and Handy[23] (N_2, CO, CH_2O, and C_2H_4) and Leang *et al.*[20] When comparing TDDFT assessments carried out on different data sets, one should keep in mind that tests on atoms and small molecules such as CH_2O tend to give larger MAEs than the same tests on larger organic molecules with π-conjugated systems. This is because TDDFT data sets for larger molecules are dominated by low-energy valence transitions that are easier to predict accurately with approximate TDDFT than for small molecules (see, e.g., the data of ref 17). As we will see, the benefits of accurate Kohn–Sham potentials are also more pronounced in tests on small systems.

4. RESULTS

A. Be atom

The beryllium atom is an ideal system for TDDFT assessments: its exact exchange-correlation potentials[60] and Kohn–Sham orbital energies[59] are known, and reliable experimental data exist.[61] In addition, the small size of this system enables one to employ large basis sets. Here we adopted the UGBS1P(3+) basis set, (28s,28p,18d), which was constructed by augmenting the UGBS1P basis set of the *Gaussian* program[49] with three primitive diffuse functions of each type following the geometric progression defined by the last two s, p, d functions of UGBS1P. This basis set is adequate for describing electron excitation of the Be atom up to the 3d level.

Figure 1 compares the LDA and PBE exchange-correlation potentials of Be to those

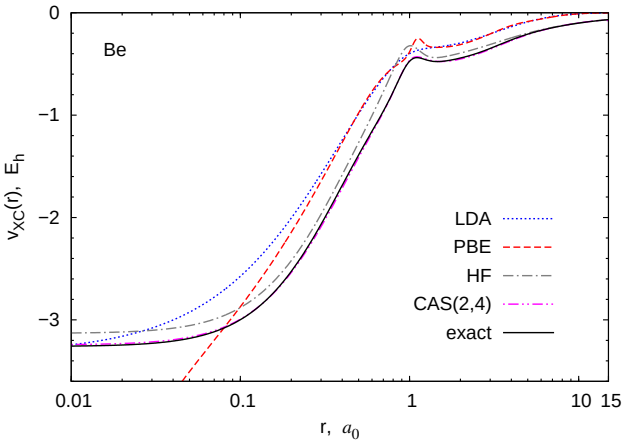

Figure 1: Exchange-correlation potentials for the Be atom generated from density-functional approximations and *ab initio* wavefunctions using the UGBS1P(3+) basis set. The exact $v_{\mathrm{XC}}(\mathbf{r})$ is from ref 60.

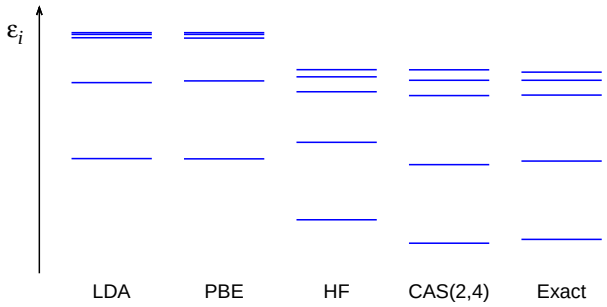

Figure 2: Energies of the $2s$, $2p$, $3s$, $3p$, and $3d$ Kohn–Sham orbitals of Be obtained from density-functional approximations and *ab initio* wavefunctions using the UGBS1P(3+) basis set. The levels are shown to scale using the data of Table S1. The exact energies are a combination of data from refs 59 and 62.

derived from the HF and full-valence CASSCF wavefunctions. The LDA and PBE potentials are not negative enough and decay too fast. As a result, the LDA and PBE Kohn–Sham spectra exhibit a characteristic collapse of Rydberg levels (Figure 2), absent in the potentials derived from the wavefunctions. The HF-based potential is essentially the exchange-only potential, whereas the potential derived from the full-valence CASSCF wavefunction is an excellent representation of the exact $v_{\mathrm{XC}}(\mathbf{r})$. Note also that the PBE potential diverges at the nucleus,[63] but this unphysical behavior does not cause any complications in TDDFT.

Table 1 demonstrates that the quality of the exchange-correlation potentials of Figure 1

Table 1: Excitation Energies (eV) of the Beryllium Atom Calculated with Adiabatic Linear-Response TDDFT Using Various Static Exchange-Correlation Potentials (First Row of the Header) and Kernels (Second Row). The Basis Set is UGBS1P(3+)

			LDA	PBE	rTPSS	PBE0	HF				CAS(2,4)			
State	Transition	Expt.	LDA	PBE	rTPSS	PBE0	LDA	PBE	rTPSS	PBE0	LDA	PBE	rTPSS	PBE0
^3P	$2s \rightarrow 2p$	2.73	2.40	1.90	1.65	1.79	2.52	1.93	0.93	−1.30	2.47	1.86	0.52	−1.39
^1P	$2s \rightarrow 2p$	5.28	4.80	4.90	5.11	4.93	4.86	4.86	4.67	3.15	5.13	5.11	4.89	3.21
^3S	$2s \rightarrow 3s$	6.46	5.52	5.42	5.74	5.68	5.75	5.66	5.77	4.62	6.64	6.55	6.65	5.46
^1S	$2s \rightarrow 3s$	6.78	5.60	5.60	5.83	5.96	6.04	6.06	6.04	5.20	6.95	6.98	6.94	6.06
^3P	$2s \rightarrow 3p$	7.29	5.71	5.71	5.92	6.18	6.46	6.34	6.39	5.45	7.38	7.25	7.32	6.31
^1P	$2s \rightarrow 3p$	7.46	5.73	5.74	5.92	6.28	6.71	6.70	6.63	5.75	7.55	7.55	7.49	6.58
^3D	$2s \rightarrow 3d$	7.69	5.80	5.81	5.97	6.42	6.84	6.69	6.81	5.78	7.79	7.61	7.72	6.59
^1D	$2s \rightarrow 3d$	7.99	5.80	5.81	6.00	6.42	6.76	6.77	6.72	5.92	7.72	7.73	7.65	6.79
MAE Valence (2)			0.41	0.60	0.62	0.65	0.31	0.61	1.21	3.08	0.21	0.52	1.30	3.10
MAE Rydberg (6)			1.59	1.60	1.38	1.12	0.85	0.91	0.89	1.82	0.15	0.13	0.13	0.98
MAE All (8)			1.29	1.35	1.19	1.00	0.72	0.83	0.97	2.14	0.16	0.22	0.42	1.51

correlates strongly with the accuracy of excitation energies predicted by TDDFT. The metric is the mean absolute error (MAE) relative to experiment. The LDA and (meta)-GGAs systematically underestimate Rydberg excitation energies (MAE=1.38–1.60 eV) because of the collapse of virtual orbitals.[31,38] The PBE0 hybrid functional gives only a modestly lower MAE for Rydberg excitations (1.12 eV) than LDA, PBE, and rTPSS.

Kohn–Sham potentials derived from HF wavefunctions are essentially exact-exchange potentials.[45,46] They have correct Coulombic ($-1/r$) decay and therefore give smaller errors for Rydberg excitation energies (MAE=0.85–0.91 eV for non-hybrid kernels) than the density-functional approximations. The improvement for valence transitions, however, is seen only for the LDA kernel (MAE=0.31 eV).

The best overall result for Be (MAE=0.16 eV) is obtained by pairing the exchange-correlation potential from the CAS(2,4) wavefunction with the LDA kernel. We have also experimented with the CAS(4,9) wavefunction but obtained the same MAEs (within 0.01 eV) as with CAS(2,4) for each kernel. It is reassuring that the CAS(2,4) results for the LDA kernel are consistent with analogous calculations of van Gisbergen *et al.*[41] who employed the exact[60] exchange-correlation potential of beryllium: individual discrepancies are small (0.05 eV to 0.18 eV) and the total MAEs for the 8 lowest transitions of Table 1 are almost identical (0.16 eV here vs. 0.15 eV in ref 41), despite the fact that van Gisbergen *et al.* used

a different basis set and a different parametrization of the LDA.

According to Table 1, wavefunction-based exchange-correlation potentials perform best for Be when paired with the LDA kernel, followed by the PBE kernel, with the rTPSS and PBE0 kernels trailing far behind. For the lowest-energy excitation, performance of the LDA, PBE, and rTPSS kernels mirrors that of the corresponding density functionals.

The PBE0 (nonlocal) kernel appears to be incompatible with multiplicative Kohn–Sham potentials: it gives implausibly low excitation energies and an imaginary value for the lowest ($2s \rightarrow 2p$) transition frequency (Table 1), which indicates a triplet instability.[64] To rationalize this observation, we recall that excitation energies of adiabatic TDDFT with pure density functionals are dominated by orbital-energy differences, whereas in the time-dependent Hartree–Fock method and in hybrid TDDFT the coupling term (contribution of the Hartree and exchange-correlation kernels) makes a large additional contribution.[59,65,66] Therefore, when the orbital energies themselves are accurate, inclusion of a significant fraction of the Hartree–Fock-type kernel makes matters worse. For this reason, from now on we will report TDDFT results obtained with wavefunction-based Kohn–Sham potentials only for the LDA, PBE, and rTPSS kernels.

B. Small molecules

Our next focus is on four small molecules: N_2, CO, CH_2O, and C_2H_4. A total of about 50 vertical excitation energies of these systems have been used for detailed assessments of adiabatic TDDFT in three previous studies relevant to this work.[23,34,38] Following these precedents, we adopted the Sadlej+ basis set and performed all calculations for the experimental equilibrium molecular geometries: $r_e = 1.098$ Å for N_2; $r_e = 1.128$ Å for CO; $r_e(\mathrm{CO}) = 1.208$ Å, $r_e(\mathrm{CH}) = 1.116$ Å, and $\theta(\mathrm{HCO}) = 121.75°$ for CH_2O; $r_e(\mathrm{CC}) = 1.339$ Å, $r_e(\mathrm{CH}) = 1.087$ Å, and $\theta(\mathrm{CCH}) = 121.3°$ for C_2H_4.

The quality of the Kohn–Sham potentials derived for these molecules from approximate density functionals and *ab initio* wavefunctions is illustrated by Figures 3 (for N_2) and 4 (for CO). As with the Be atom, the wavefunctions yield significantly more realistic potentials than do the LDA and PBE functionals. Of course, full-valence CASSCF wavefunctions are not exact and, in the absence of exact benchmarks, we do not know how accurate the full-valence CASSCF potentials of Figures 3 and 4 actually are. What we do know is

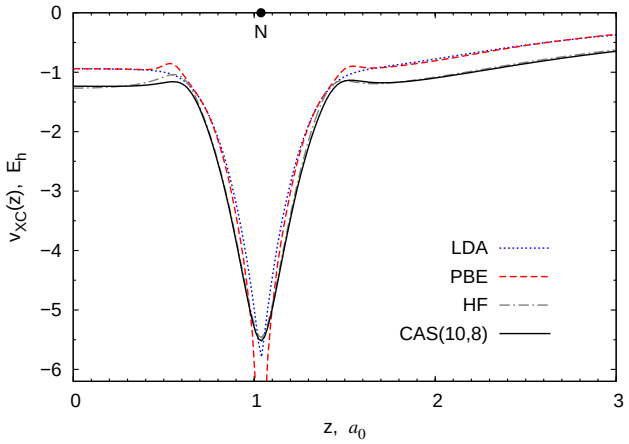

Figure 3: Exchange-correlation potentials for N_2 generated from density-functional approximations, HF, and full-valence CASSCF wavefunctions using the Sadlej+ basis set. The plots show potentials along the internuclear axis with the bond midpoint at $z = 0$.

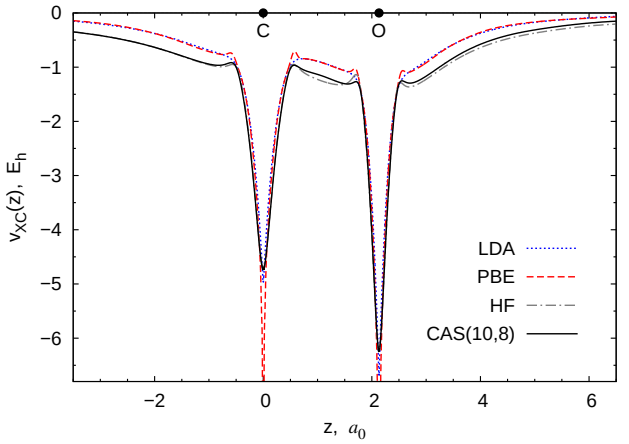

Figure 4: Exchange-correlation potentials for CO generated from density-functional approximations, HF, and full-valence CASSCF wavefunctions using the Sadlej+ basis set.

that exchange-correlation potentials obtained by our method for atoms and small molecules converge with respect to the level of theory quite rapidly, at least visually (see, for instance, Figure 1 and ref 67). This suggests that the full-valence CASSCF potentials of Figures 3 and 4 must be very close to the exact $v_X(\mathbf{r})$ and $v_{XC}(\mathbf{r})$, respectively. In any case, improvement of these potentials beyond the full-valence CASSCF level should not lead to substantially different TDDFT results for small molecules such as N_2 and CO.

Tables 2–5 show details and summaries of TDDFT results for N_2, CO, CH_2O, and C_2H_4. The trends here are similar to those observed for the Be atom: density-functional approxi-

Table 2: Same as in Table 1 for the N_2 Molecule Using the Sadlej+ Basis Set

			LDA	PBE	rTPSS	PBE0	HF			CAS(10,8)		
State	Transition	Expt.	LDA	PBE	rTPSS	PBE0	LDA	PBE	rTPSS	LDA	PBE	rTPSS
$^3\Sigma_u^+$	$\pi_u \rightarrow \pi_g$	7.75	7.86	7.51	7.31	6.93	8.48	8.09	7.59	8.01	7.62	7.09
$^3\Pi_g$	$\sigma_g \rightarrow \pi_g$	8.04	7.54	7.37	7.52	7.50	8.58	8.30	7.97	8.04	7.75	7.42
$^3\Delta_u$	$\pi_u \rightarrow \pi_g$	8.88	8.82	8.31	8.18	7.90	9.37	8.86	8.45	8.96	8.43	7.99
$^1\Pi_g$	$\sigma_g \rightarrow \pi_g$	9.31	9.04	9.08	9.31	9.31	10.13	10.06	9.84	9.59	9.52	9.30
$^3\Sigma_u^-$	$\pi_u \rightarrow \pi_g$	9.67	9.64	9.66	9.93	9.34	10.16	10.16	10.16	9.79	9.79	9.79
$^1\Sigma_u^-$	$\pi_u \rightarrow \pi_g$	9.92	9.64	9.66	9.93	9.34	10.16	10.16	10.16	9.79	9.79	9.79
$^1\Delta_u$	$\pi_u \rightarrow \pi_g$	10.27	10.22	10.08	10.05	9.89	10.70	10.56	10.26	10.37	10.22	9.92
$^3\Pi_u$	$\sigma_u \rightarrow \pi_g$	11.19	10.36	10.38	10.76	10.74	11.34	11.06	10.73	11.01	10.72	10.39
$^3\Sigma_g^+$	$\sigma_g \rightarrow 3s\sigma_g$	12.0	10.28	10.06	10.32	11.17	11.72	11.67	11.67	11.54	11.51	11.51
$^1\Sigma_g^+$	$\sigma_g \rightarrow 3s\sigma_g$	12.2	10.39	10.23	10.43	11.47	11.94	11.94	11.94	11.61	11.61	11.61
$^1\Pi_u$	$\sigma_g \rightarrow 3p\pi_u$	12.90	10.98	10.80	11.03	11.99	12.47	12.47	12.47	11.96	11.96	11.96
$^1\Sigma_u^+$	$\sigma_g \rightarrow 3p\sigma_u$	12.98	10.62	10.48	10.66	11.87	12.59	12.59	12.59	12.14	12.14	12.14
$^1\Pi_u$	$\pi_u \rightarrow 3s\sigma_g$	13.24	11.80	11.53	11.58	12.32	12.75	12.76	12.74	12.68	12.68	12.68
MAE Valence (8)			0.27	0.37	0.32	0.51	0.49	0.32	0.30	0.14	0.23	0.45
MAE Rydberg (5)			1.85	2.04	1.86	0.90	0.37	0.38	0.38	0.68	0.68	0.68
MAE All (13)			0.88	1.02	0.91	0.66	0.44	0.34	0.33	0.35	0.41	0.54

mations perform reasonably well for valence excitations (with MAEs typically in 0.2–0.4 eV range) but poorly for Rydberg transitions (with most MAEs falling between 1 and 2 eV). Exchange-only potentials perform much better for Rydberg transitions but not for valence excitations. Exchange-correlation potentials derived from full-valence CASSCF wavefunctions produce results that are best overall. The lowest MAEs for valence transitions are 0.14 eV for N_2 and CO (using the LDA kernel), 0.22 eV for CH_2O (rTPSS kernel), and 0.10 eV for C_2H_4 (PBE kernel). One the other hand, the MAEs of Rydberg transitions are higher for CASSCF-based potentials than for HF wavefunctions in three cases out of four (N_2, CO, and C_2H_4). This surprising outcome may be an artifact of the sensitivity of Rydberg excitation energies to the choice of diffuse functions. Another possibly contributing factor

Table 3: Same as in Table 1 for the CO Molecule Using the Sadlej+ Basis Set

			LDA	PBE	rTPSS	PBE0	HF			CAS(10,8)		
State	Transition	Expt.	LDA	PBE	rTPSS	PBE0	LDA	PBE	rTPSS	LDA	PBE	rTPSS
$^3\Pi$	$\sigma \rightarrow \pi^*$	6.32	5.96	5.73	5.87	5.73	6.69	6.25	5.78	6.49	6.08	5.64
$^3\Sigma^+$	$\pi \rightarrow \pi^*$	8.51	8.39	8.09	8.02	7.84	9.39	9.09	8.72	8.56	8.24	7.83
$^1\Pi$	$\sigma \rightarrow \pi^*$	8.51	8.18	8.25	8.52	8.44	9.09	9.03	8.78	8.75	8.69	8.44
$^3\Delta$	$\pi \rightarrow \pi^*$	9.36	9.17	8.74	8.72	8.61	10.09	9.68	9.38	9.32	8.88	8.55
$^3\Sigma^-$	$\pi \rightarrow \pi^*$	9.88	9.85	9.84	10.12	9.78	10.71	10.71	10.71	9.99	9.99	9.99
$^1\Sigma^-$	$\pi \rightarrow \pi^*$	9.88	9.85	9.84	10.12	9.78	10.71	10.71	10.71	9.99	9.99	9.99
$^1\Delta$	$\pi \rightarrow \pi^*$	10.23	10.32	10.18	10.21	10.20	11.13	11.00	10.77	10.46	10.33	10.08
$^3\Sigma^+$	$\sigma \rightarrow 3s$	10.4	8.96	8.79	9.12	9.70	10.53	10.46	10.45	10.81	10.73	10.73
$^1\Sigma^+$	$\sigma \rightarrow 3s$	10.78	9.07	8.98	9.25	10.05	10.92	10.92	10.90	11.31	11.32	11.29
$^3\Sigma^+$	$\sigma \rightarrow 3p\sigma$	11.3	9.33	9.25	9.50	10.35	11.65	11.51	10.57	11.72	11.60	11.65
$^1\Sigma^+$	$\sigma \rightarrow 3p\sigma$	11.40	9.35	9.25	9.53	10.42	11.84	11.90	11.85	11.88	11.92	11.86
$^3\Pi$	$\sigma \rightarrow 3p\pi$	11.53	9.49	9.41	9.68	10.49	11.89	11.90	11.88	12.14	12.15	12.12
$^1\Pi$	$\sigma \rightarrow 3p\pi$	11.55	9.48	9.36	9.62	10.43	11.84	11.75	11.78	12.10	12.00	12.03
$^1\Sigma^+$	$\sigma \rightarrow 3d\sigma$	12.4	9.94	9.84	10.11	11.05	13.09	13.11	13.05	13.35	13.35	13.26
MAE Valence (7)			0.16	0.29	0.30	0.33	0.73	0.56	0.46	0.14	0.21	0.37
MAE Rydberg (7)			1.96	2.07	1.79	0.98	0.34	0.31	0.37	0.56	0.53	0.51
MAE All (14)			1.06	1.18	1.05	0.66	0.54	0.44	0.42	0.35	0.37	0.44

is that potentials generated by our method sometimes deviate from the correct asymptotic $-1/r$ decay beyond a certain large r when the basis set contains very diffuse basis functions.

Inspection of Tables 2–5 reveals another limitation of replacing density-functional approximations for $v_{\mathrm{XC}}(\mathbf{r})$ with accurate exchange-correlation potentials while keeping approximate kernels. According to Figures 3 and 4, molecular exchange-correlation potentials derived from HF and full-valence CASSCF wavefunctions are not substantially different, at least visually. However, they produce distinct excitation energies for a fixed exchange-correlation kernel, with MAEs differing by up to 0.7 eV (Tables 2–5). These differences are greater on average than the differences between the MAEs of the LDA, PBE, and rTPSS density-

Table 4: Same as in Table 1 for the CH_2O Molecule Using the Sadlej+ Basis Set

			LDA	PBE	rTPSS	PBE0	HF			CAS(12,10)		
State	Transition	Expt.	LDA	PBE	rTPSS	PBE0	LDA	PBE	rTPSS	LDA	PBE	rTPSS
$^3A_2$	$n \rightarrow \pi^*$	3.50	3.05	3.05	3.29	3.13	4.43	4.26	4.05	3.68	3.51	3.29
$^1A_2$	$n \rightarrow \pi^*$	3.94	3.66	3.78	4.09	3.92	5.01	4.97	4.82	4.29	4.24	4.10
$^3A_1$	$\pi \rightarrow \pi^*$	5.53	6.18	5.75	5.63	5.22	6.97	6.55	6.18	6.48	6.02	5.62
$^3B_2$	$n \rightarrow 3sa_1$	6.83	5.76	5.58	5.88	6.46	7.65	7.55	7.46	7.11	6.99	6.89
$^1B_2$	$n \rightarrow 3sa_1$	7.09	5.82	5.73	5.97	6.66	7.78	7.80	7.75	7.30	7.32	7.27
$^3A_1$	$n \rightarrow 3pb_2$	7.79	6.37	6.25	6.42	7.75	8.85	8.75	8.73	8.33	8.22	8.20
$^1A_1$	$n \rightarrow 3pb_2$	7.97	6.37	6.29	6.43	7.38	8.98	9.00	8.97	8.48	8.51	8.47
$^3B_2$	$n \rightarrow 3pa_1$	7.96	6.38	6.30	6.43	7.60	8.43	8.35	8.29	8.08	8.00	7.97
$^1B_2$	$n \rightarrow 3pa_1$	8.12	6.38	6.32	6.44	7.63	8.64	8.65	8.60	8.25	8.26	8.20
$^1B_1$	$\sigma \rightarrow \pi^*$	8.38	6.56	6.48	6.62	7.55	8.90	8.91	8.90	9.20	9.21	9.20
$^1A_2$	$n \rightarrow 3pb_1$	8.68	8.74	8.79	9.10	9.08	9.98	9.93	9.79	9.30	9.24	9.09
$^1A_2$	$n \rightarrow 3db_1$	9.22	7.10	7.02	7.15	8.13	10.69	10.69	10.68	10.96	10.97	10.95
MAE Valence (4)			0.36	0.23	0.22	0.28	1.19	1.01	0.80	0.53	0.34	0.22
MAE Rydberg (8)			1.58	1.67	1.50	0.53	0.82	0.79	0.75	0.54	0.52	0.47
MAE All (12)			1.17	1.19	1.07	0.44	0.94	0.87	0.77	0.54	0.46	0.39

functional approximations. This fact highlights the risk of relying on accurate Kohn–Sham potentials when exchange-correlation kernels remain approximate. It is also notable that, for a given *ab initio* Kohn–Sham potential, the LDA, PBE, and rTPSS kernels give practically identically results for the high-energy transitions, whereas the predicted energies of the low-energy transitions strongly depend on the kernel.

When the results for Be and the four molecules of this section are combined (Table 6), TDDFT with Kohn–Sham potentials derived from full-valence CASSCF wavefunctions emerges as a clear winner with the overall MAEs of 0.41 eV and 0.31 eV for the LDA and PBE kernels, respectively. These errors are 2–3 times lower than the MAEs of the density-functional approximations including PBE0.

The results for the Be atom, N_2, CO, CH_2O, and C_2H_4 suggest that Kohn–Sham po-

Table 5: Same as in Table 1 for the C_2H_4 Molecule Using the Sadlej+ Basis Set

	Excited		LDA	PBE	rTPSS	PBE0	HF			CAS(12,12)		
State	Orbital	Expt.	LDA	PBE	rTPSS	PBE0	LDA	PBE	rTPSS	LDA	PBE	rTPSS
$^3B_{1u}$	π^*	4.36	4.62	4.20	4.11	3.79	5.07	4.64	4.26	4.82	4.35	3.91
$^3B_{3u}$	$3s$	6.98	6.49	6.26	6.39	6.67	7.05	6.98	7.02	7.49	7.44	7.45
$^1B_{3u}$	$3s$	7.11	6.53	6.35	6.42	6.79	7.14	7.17	7.13	7.60	7.62	7.59
$^3B_{1g}$	$3p\pi$	7.79	6.90	6.71	6.72	7.72	8.00	7.95	7.95	8.24	8.18	8.16
$^1B_{1g}$	$3p\pi$	7.80	6.91	6.73	6.73	7.73	8.01	8.02	7.99	8.36	8.35	8.31
$^1B_{2g}$	$3p\sigma$	7.90	6.91	6.73	6.72	7.72	8.04	8.05	8.04	8.32	8.33	8.31
$^1B_{1u}$	π^*	8.0	7.30	7.47	7.54	7.45	7.73	7.69	7.54	7.87	7.82	7.65
^3A_g	$3p\pi$	8.15	7.13	6.91	6.91	7.44	7.92	7.82	7.88	8.74	8.66	8.72
^1A_g	$3p\pi$	8.28	7.15	6.97	6.95	7.55	8.07	8.09	8.07	8.90	8.93	8.91
$^3B_{3u}$	$3d\sigma$	8.57	6.97	6.80	6.77	7.60	8.60	8.49	8.50	9.08	8.98	8.99
$^1B_{3u}$	$3d\sigma$	8.62	6.97	6.81	6.78	7.62	8.71	8.71	8.68	9.23	9.24	9.19
$^1B_{3u}$	$3d\delta$	8.90	7.35	7.19	7.17	7.89	9.26	9.27	9.25	9.69	9.70	9.67
$^1B_{2u}$	$3d\delta$	9.05	7.44	7.27	7.24	7.96	8.95	8.96	8.93	9.83	9.84	9.81
$^1B_{1u}$	$3d\pi$	9.33	7.58	7.17	7.18	8.04	9.53	9.51	9.48	10.23	10.22	10.19
MAE Valence (2)			0.48	0.35	0.35	0.56	0.49	0.29	0.28	0.29	0.10	0.40
MAE Rydberg (12)			1.18	1.38	1.38	0.65	0.16	0.16	0.15	0.60	0.58	0.57
MAE All (14)			1.08	1.23	1.23	0.63	0.20	0.18	0.17	0.56	0.51	0.54

Table 6: MAEs (eV) for the Combined Data of Tables 1–5. See the Abstract Graphic for Visualization

	v_{XC}:	LDA	PBE	rTPSS	PBE0	HF			Full-valence CASSCF		
Property	f_{XC}:	LDA	PBE	rTPSS	PBE0	LDA	PBE	rTPSS	LDA	PBE	rTPSS
Valence (23)		0.36	0.42	0.38	0.45	0.63	0.50	0.49	0.23	0.27	0.47
Rydberg (38)		1.51	1.64	1.51	0.78	0.49	0.49	0.48	0.52	0.49	0.47
All (61)		1.08	1.18	1.08	0.65	0.54	0.49	0.48	0.41	0.31	0.47

Table 7: MAEs (eV) for the Test Set of 101 Excitation Energies of Ref 20 Computed with Standard Exchange-Correlation Functionals and Kohn–Sham Potentials Derived from HF Wavefunctions. The Basis Set is 6-311++G(3df,3pd)

	v_{XC}:	LDA	PBE	rTPSS	PBE0	HF		
Property	f_{XC}:	LDA	PBE	rTPSS	PBE0	LDA	PBE	rTPSS
Valence (60)		0.49	0.44	0.31	0.29	0.48	0.40	0.33
Rydberg (41)		0.60	0.78	0.59	0.24	0.49	0.48	0.45
All (101)		0.53	0.58	0.42	0.27	0.48	0.43	0.38

tentials derived from HF wavefunctions (i.e., exchange-only potentials) perform consistently better than standard density-functional approximations only for Rydberg excitations, but not for valence transitions (Table 6). To ascertain whether this result is general, we extended our tests of HF-based Kohn–Sham potentials to a larger test set.

C. Larger molecules

The test set of Leang *et al.*[20] consists of 101 excitation energies (60 valence and 41 Rydberg transitions) of 14 molecules (benzene, butadiene, cyclopentadiene, ethylene, formaldehyde, furan, methylenecyclopropene, pyrazine, pyridine, pyrrole, *s*-tetrazine, *s-trans*-acrolein, *s-trans*-glyoxal, and water). Following Leang *et al.*,[20] we used the 6-311++G(3df,3pd) basis set for all calculations on this test set. In contrast to ref 20, however, we did not reoptimize molecular geometries with each functional but used the PBE0/6-311++G(3df,3pd) geometries for all TDDFT calculations, to disentangle the effect of geometry relaxation from the accuracy of the potential. Note that two molecules of the set, CH_2O and C_2H_4, are the same as in section 4 B, but we did not exclude them because the methodology (basis set, number of excitations, and sources of experimental data) of the present section is different.

The results are summarized in Table 7 and details for individual excitations are given in the Supporting Information (Table S2). In agreement with sections 4 A and 4 B, use of Kohn–Sham potentials derived from HF wavefunctions improves Rydberg excitation energies but has little effect on the accuracy of valence excitations. The fact that this conclusion has been reached for different systems and different basis sets makes it quite certain.

As in section 4 B, Kohn–Sham potentials derived from HF wavefunctions (MAE=0.38–0.48 eV) perform better than the LDA, PBE, and rTPSS exchange-correlation functionals (MAE=0.42–0.58 eV), but this time not quite as well as PBE0 (MAE=0.27 eV). The PBE0 functional is no ordinary contender: Leang *et al.*[20] found that it has the best overall accuracy in TDDFT among 24 diverse density functionals. Nevertheless, we believe that the much better performance of PBE0 in Table 7 than in Table 6 has to do with the 6-311++G(3df,3pd) basis set which lacks highly diffuse functions of Sadlej+. The absence of such functions artificially props up Rydberg states and make PBE0 appear more accurate than it actually is. Comparison of Tables 6 and 7 suggests that Rydberg excitation energies computed with asymptotically correct potentials are less sensitive to the basis set than the same excitations computed with standard density functionals, and that Kohn–Sham potentials derived from wavefunctions would outperform PBE0 closer to the basis-set limit (Table 6).

5. CONCLUSIONS

We have presented numerical tests of adiabatic linear-response TDDFT in which Kohn–Sham orbitals and orbital energies derived from HF and post-HF wavefunctions are paired with standard density-functional approximations for the static exchange-correlation kernel. Our main findings are as follows.

(1) Accurate exchange-correlation potentials combined with approximate exchange-correlation kernels generally perform much better than standard density-functional approximations, provided that the kernels are derived from local or semilocal (not hybrid) functionals.

(2) Kohn–Sham potentials derived from HF wavefunctions give better results than local and semilocal exchange-correlation functionals for Rydberg excitations, but not for valence transitions. To outperform standard density functionals with wavefunction-based potentials, one needs post-HF wave functions.

(3) For a fixed Kohn–Sham potential derived from a wavefunction, variation of the static kernel from LDA to PBE to rTPSS causes substantial changes in predicted excitation energies for low-lying states, but makes very little difference for Rydberg states.

(4) Hybrid kernels such as PBE0 are not compatible with multiplicative exchange-correlation potentials.

(5) Advantages of accurate Kohn–Sham potentials over standard density-functional approximations may vanish in TDDFT calculations using insufficiently large basis sets.

It is unlikely that the lowest MAEs reported in this work for valence excitations (0.15–0.2 eV) can be further reduced by improving static Kohn–Sham potentials alone. This is because (i) potentials derived from full-valence CASSCF wavefunctions are already quite accurate; (ii) the calculated valence excitation energies change appreciably in response to variations in exchange-correlation kernels; (iii) previous applications of accurate Kohn–Sham potentials in TDDFT[29,31,33,34,42] were unable to reduce the MAE consistently below 0.2 eV, even when the potentials were exact.[33] Errors for Rydberg excitations are even more difficult to reduce below 0.4 eV. Thus, it appears that the practical accuracy limit of adiabatic linear-response TDDFT with exact exchange-correlation potentials and standard density-functional kernels is 0.15–0.2 eV. For large basis sets, this accuracy is better than that of the best-performing (hybrid) density functionals such as PBE0.

It would be interesting to investigate whether our estimate of this limit can be pushed even further by using exchange-correlation kernels derived from meta-GGAs with a stronger dependence on kinetic energy density than that of (rev)TPSS, and by differentiating the functional with respect to $\rho(\mathbf{r})$ rather than Kohn–Sham orbitals.[68] Regardless of the outcome, accuracy of TDDFT can be improved continuously by devising more accurate models for the static exchange-correlation kernel or by going beyond the adiabatic approximation.

Acknowledgments

The work was supported by the Natural Sciences and Engineering Research Council (NSERC) of Canada through a Discovery Grant (Application No. RGPIN-2015-04814) and a Discovery Accelerator Supplement (RGPAS 477791-2015).

Supporting Information

The Supporting Information is available free of charge on the ACS Publications website at DOI: 10.1021/acs.jctc.xxxxxxx

Calculated Kohn–Sham orbital energies of the Be atom, calculated excitation energies for the test set of Leang and co-workers, total electronic energies from the HF and CASSCF wavefunctions used for generating the potentials (PDF)

REFERENCES

[1] Elliott, P.; Furche, F.; Burke, K. Excited states from time-dependent density functional theory. *Rev. Comput. Chem.* **2009**, *26*, 91–165.

[2] Gross, E. K. U.; Maitra, N. T. In *Fundamentals of Time-Dependent Density Functional Theory*; Marques, M. A. L., Maitra, N. T., Nogueira, F. M. S., Gross, E. K. U., Rubio, A., Eds.; Springer: Berlin, 2012; pp 53–99.

[3] Ullrich, C. A. *Time-Dependent Density-Functional Theory. Concepts and Applications*; Oxford University Press: Oxford, 2012.

[4] Petersilka, M.; Gossmann, U. J.; Gross, E. K. U. Excitation energies from time-dependent density-functional theory. *Phys. Rev. Lett.* **1996**, *76*, 1212–1215.

[5] Casida, M. E. In *Recent Advances in Density Functional Methods, Part I*; Chong, D. P., Ed.; World Scientific: Singapore, 1995; pp 155–192.

[6] Bauernschmitt, R.; Ahlrichs, R. Treatment of electronic excitations within the adiabatic approximation of time dependent density functional theory. *Chem. Phys. Lett.* **1996**, *256*, 454–464.

[7] Stratmann, R. E.; Scuseria, G. E.; Frisch, M. J. An efficient implementation of time-dependent density-functional theory for the calculation of excitation energies of large molecules. *J. Chem. Phys.* **1998**, *109*, 8218–8224.

[8] Jamorski, C.; Casida, M. E.; Salahub, D. R. Dynamic polarizabilities and excitation spectra from a molecular implementation of time-dependent density-functional response theory: N_2 as a case study. *J. Chem. Phys.* **1996**, *104*, 5134–5147.

[9] Hirata, S.; Head-Gordon, M. Time-dependent density functional theory for radicals: An improved description of excited states with substantial double excitation character. *Chem. Phys. Lett.* **1999**, *302*, 375–382.

[10] Ziegler, T.; Seth, M.; Krykunov, M.; Autschbach, J.; Wang, F. On the relation between time-dependent and variational density functional theory approaches for the determination of excitation energies and transition moments. *J. Chem. Phys.* **2009**, *130*, 154102.

[11] Thiele, M.; Kümmel, S. Photoabsorption spectra from adiabatically exact time-dependent density-functional theory in real time. *Phys. Chem. Chem. Phys.* **2009**, *11*, 4631–4639.

[12] Ciofini, I.; Adamo, C. Accurate evaluation of valence and low-lying Rydberg states with standard time-dependent density functional theory. *J. Phys. Chem. A* **2007**, *111*, 5549–5556.

[13] Rohrdanz, M. A.; Herbert, J. M. Simultaneous benchmarking of ground- and excited-state properties with long-range-corrected density functional theory. *J. Chem. Phys.* **2008**, *129*, 034107.

[14] Silva-Junior, M. S.; Schreiber, M.; Sauer, S. P. A.; Thiel, W. Benchmarks for electronically excited states: Time-dependent density functional theory and density functional theory based multireference configuration interaction. *J. Chem. Phys.* **2008**, *129*, 104103.

[15] Jacquemin, D.; Wathelet, V.; Perpète, E. A.; Adamo, C. Extensive TD-DFT benchmark: Singlet-excited states of organic molecules. *J. Chem. Theory Comput.* **2009**, *5*, 2420–2435.

[16] Jacquemin, D.; Perpète, E. A.; Ciofini, I.; Adamo, C. Assessment of functionals for TD-DFT calculations of singlet–triplet transitions. *J. Chem. Theory Comput.* **2010**, *6*, 1532–1537.

[17] Caricato, M.; Trucks, G. W.; Frisch, M. J.; Wiberg, K. B. Electronic transition energies: A study of the performance of a large range of single reference density functional and wave function methods on valence and Rydberg states compared to experiment. *J. Chem. Theory Comput.* **2012**, *6*, 370–383.

[18] Send, R.; Kühn, M.; Furche, F. Assessing excited state methods by adiabatic excitation energies. *J. Chem. Theory Comput.* **2011**, *7*, 2376–2386.

[19] Yang, K.; Peverati, R.; Truhlar, D. G.; Valero, R. Density functional study of multiplicity-changing valence and Rydberg excitations of p-block elements: Delta self-consistent field, collinear spin-flip time-dependent density functional theory (DFT), and conventional time-dependent DFT. *J. Chem. Phys.* **2011**, *135*, 044118.

[20] Leang, S. S.; Zahariev, F.; Gordon, M. S. Benchmarking the performance of time-dependent density functional methods. *J. Chem. Phys.* **2012**, *136*, 104101.

[21] Momeni, M. R.; Brown, A. Why do TD-DFT excitation energies of BODIPY/aza-BODIPY families largely deviate from experiment? Answers from electron correlated and multireference methods. *J. Chem. Theory Comput.* **2015**, *11*, 2619–2632.

[22] Brémond, E.; Savarese, M.; Pérez-Jiménez, A. J.; Sancho-García, J. C.; Adamo, C. Speed-up of the excited-state benchmarking: Double-hybrid density functionals as test cases. *J. Chem. Theory Comput.* **2017**, *13*, 5539–5551.

[23] Tozer, D. J.; Handy, N. C. Improving virtual Kohn–Sham orbitals and eigenvalues: Application to excitation energies and static polarizabilities. *J. Chem. Phys.* **1998**, *109*, 10180–10189.

[24] Casida, M. E.; Salahub, D. R. Asymptotic correction approach to improving approximate exchange-correlation potentials: Time-dependent density-functional theory calculations of molecular excitation spectra. *J. Chem. Phys.* **2000**, *113*, 8918–8935.

[25] Gaiduk, A. P.; Firaha, D. S.; Staroverov, V. N. Improved electronic excitation energies from shape-corrected semilocal Kohn–Sham potentials. *Phys. Rev. Lett.* **2012**, *108*, 253005.

[26] Gaiduk, A. P.; Mizzi, D.; Staroverov, V. N. Self-interaction correction scheme for approximate Kohn–Sham potentials. *Phys. Rev. A* **2012**, *86*, 052518.

[27] Li, S. L.; Truhlar, D. G. Testing time-dependent density functional theory with depopulated molecular orbitals for predicting electronic excitation energies of valence, Rydberg, and charge-transfer states and potential energies near a conical intersection. *J. Chem. Phys.* **2014**, *141*, 104106.

[28] Komsa, D. N.; Staroverov, V. N. Do fractionally incremented nuclear charges improve time-dependent density functional theory excitation energies as reliably as fractional orbital populations? *Theor. Chem. Acc.* **2017**, *136*, 101.

[29] Baerends, E. J.; Gritsenko, O. V.; van Meer, R. The Kohn–Sham gap, the fundamental gap and the optical gap: The physical meaning of occupied and virtual Kohn–Sham orbital energies. *Phys. Chem. Chem. Phys.* **2013**, *15*, 16408–16425.

[30] van Gisbergen, S. J. A.; Osinga, V. P.; Gritsenko, O. V.; van Leeuwen, R.; Snijders, J. G.; Baerends, E. J. Improved density functional theory results for frequency-dependent polarizabilities, by the use of an exchange-correlation potential with correct asymptotic behavior. *J. Chem. Phys.* **1996**, *105*, 3142–3151.

[31] van Meer, R.; Gritsenko, O. V.; Baerends, E. J. Physical meaning of virtual Kohn–Sham orbitals and orbital energies: An ideal basis for the description of molecular excitations. *J. Chem. Theory Comput.* **2014**, *10*, 4432–4441.

[32] Petersilka, M.; Gossmann, U. J.; Gross, E. K. U. In *Electronic Density Functional Theory. Recent Progress and New Directions*; Dobson, J. F., Vignale, G., Das, M. P., Eds.; Plenum: New York, 1998; pp 177–197.

[33] Bleiziffer, P.; Heßelmann, A.; Umrigar, C. J.; Görling, A. Influence of the exchange-correlation potential in methods based on time-dependent density-functional theory. *Phys. Rev. A* **2013**,

88, 042513.

[34] Wu, Q.; Cohen, A. J.; Yang, W. Excitation energies from time-dependent density functional theory with accurate exchange-correlation potentials. *Mol. Phys.* **2005**, *103*, 711–717.

[35] Hirata, S.; Ivanov, S.; Grabowski, I.; Bartlett, R. J. Time-dependent density functional theory employing optimized effective potentials. *J. Chem. Phys.* **2002**, *116*, 6468–6481.

[36] Kümmel, S.; Kronik, L. Orbital-dependent density functionals: Theory and applications. *Rev. Mod. Phys.* **2008**, *80*, 3–60.

[37] Heßelmann, A.; Görling, A. Efficient exact-exchange time-dependent density-functional theory methods and their relation to time-dependent Hartree–Fock. *J. Chem. Phys.* **2011**, *134*, 034120.

[38] Casida, M. E.; Jamorski, C.; Casida, K. C.; Salahub, D. R. Molecular excitation energies to high-lying bound states from time-dependent density-functional response theory: Characterization and correction of the time-dependent local density approximation ionization threshold. *J. Chem. Phys.* **1998**, *108*, 4439–4449.

[39] Schipper, P. R. T.; Gritsenko, O. V.; van Gisbergen, S. J. A.; Baerends, E. J. Molecular calculations of excitation energies and (hyper)polarizabilities with a statistical average of orbital model exchange-correlation potentials. *J. Chem. Phys.* **2000**, *112*, 1344–1352.

[40] Gaiduk, A. P.; Staroverov, V. N. Virial exchange energies from model exact-exchange potentials. *J. Chem. Phys.* **2008**, *128*, 204101.

[41] van Gisbergen, S. J. A.; Kootstra, F.; Schipper, P. R. T.; Gritsenko, O. V.; Snijders, J. G.; Baerends, E. J. Density-functional-theory response-property calculations with accurate exchange-correlation potentials. *Phys. Rev. A* **1998**, *57*, 2556–2571.

[42] Allen, M. J.; Tozer, D. J. Polarizabilities and excitation energies from the multiplicative Kohn–Sham (MKS) approach. *Mol. Phys.* **2003**, *101*, 421–425.

[43] Jin, Y.; Yang, Y.; Zhang, D.; Peng, D.; Yang, W. Improved density functional theory results for frequency-dependent polarizabilities, by the use of an exchange-correlation potential with correct asymptotic behavior. *J. Chem. Phys.* **2017**, *147*, 134105.

[44] Ryabinkin, I. G.; Kananenka, A. A.; Staroverov, V. N. Accurate and efficient approximation to the optimized effective potential for exchange. *Phys. Rev. Lett.* **2013**, *111*, 013001.

[45] Kohut, S. V.; Ryabinkin, I. G.; Staroverov, V. N. Hierarchy of model Kohn–Sham potentials for orbital-dependent functionals: A practical alternative to the optimized effective potential method. *J. Chem. Phys.* **2014**, *140*, 18A535.

[46] Ryabinkin, I. G.; Kohut, S. V.; Staroverov, V. N. Reduction of electronic wavefunctions to Kohn–Sham effective potentials. *Phys. Rev. Lett.* **2015**, *115*, 083001.

[47] Cuevas-Saavedra, R.; Ayers, P. W.; Staroverov, V. N. Kohn–Sham exchange-correlation potentials from second-order reduced density matrices. *J. Chem. Phys.* **2015**, *143*, 244116.

[48] Ospadov, E.; Ryabinkin, I. G.; Staroverov, V. N. Improved method for generating exchange-correlation potentials from electronic wave functions. *J. Chem. Phys.* **2017**, *146*, 084103.

[49] Frisch, M. J.; Trucks, G. W.; Schlegel, H. B.; Scuseria, G. E.; Robb, M. A.; Cheeseman, J. R.; Scalmani, G.; Barone, V.; Petersson, G. A.; Nakatsuji, H.; et al. *Gaussian Development Version, Revision I.13*; Gaussian, Inc.: Wallingford, CT, 2016.

[50] Perdew, J. P.; Schmidt, K. In *Density Functional Theory and Its Application to Materials*; Van Doren, V., Van Alsenoy, C., Geerlings, P., Eds.; AIP: Melville, NY, 2001; pp 1–20.

[51] Perdew, J. P.; Ruzsinszky, A.; Tao, J.; Staroverov, V. N.; Scuseria, G. E.; Csonka, G. I. Prescription for the design and selection of density functional approximations: More constraint satisfaction with fewer fits. *J. Chem. Phys.* **2005**, *123*, 062201.

[52] Perdew, J. P.; Wang, Y. Accurate and simple analytic representation of the electron-gas correlation energy. *Phys. Rev. B* **1992**, *45*, 13244–13249.

[53] Perdew, J. P.; Burke, K.; Ernzerhof, M. Generalized gradient approximation made simple. *Phys. Rev. Lett.* **1996**, *77*, 3865–3868.

[54] Perdew, J. P.; Ruzsinszky, A.; Csonka, G. I.; Constantin, L. A.; Sun, J. Workhorse semilocal density functional for condensed matter physics and quantum chemistry. *Phys. Rev. Lett.* **2009**, *103*, 026403.

[55] Ernzerhof, M.; Scuseria, G. E. Assessment of the Perdew–Burke–Ernzerhof exchange-correlation functional. *J. Chem. Phys.* **1999**, *110*, 5029–5036.

[56] Adamo, C.; Scuseria, G. E.; Barone, V. Accurate excitation energies from time-dependent density functional theory: Assessing the PBE0 model. *J. Chem. Phys.* **1999**, *111*, 2889–2899.

[57] Sadlej, A. J. Medium-size polarized basis for high-level correlated calculations of molecular electric properties. *Coll. Czech. Chem. Commun.* **1988**, *53*, 1995–2016.

[58] Schuchardt, K. L.; Didier, B. T.; Elsethagen, T.; Sun, L.; Gurumoorthi, V.; Chase, J.; Li, J.; Windus, T. L. Basis set exchange: A community database for computational sciences. *J. Chem. Inf. Model.* **2007**, *47*, 1045–1052.

[59] Savin, A.; Umrigar, C. J.; Gonze, X. Relationship of Kohn-Sham eigenvalues to excitation

energies. *Chem. Phys. Lett.* **1998**, *288*, 391–395.

[60] Filippi, C.; Gonze, X.; Umrigar, C. J. In *Recent Developments and Applications of Modern Density Functional Theory*; Seminario, J. M., Ed.; Elsevier: Amsterdam, 1996; pp 295–326.

[61] Bashkin, S.; Stoner, J. O. *Atomic Energy Levels and Grotrian Diagrams. 1. Hydrogen I—Phosphorus XV*; North Holland: Amsterdam, 1975; Vol. 1.

[62] Chakravorty, S. J.; Gwaltney, S. R.; Davidson, E. R.; Parpia, F. A.; Froese Fischer, C. Ground-state correlation energies for atomic ions with 3 to 18 electrons. *Phys. Rev. A* **1993**, *47*, 3649–3670.

[63] Umrigar, C. J.; Gonze, X. Accurate exchange-correlation potentials and total-energy components for the helium isoelectronic series. *Phys. Rev. A* **1994**, *50*, 3827–3837.

[64] Cordova, F.; Joubert Doriol, L.; Ipatov, A.; Casida, M. E.; Filippi, C.; Vela, A. Troubleshooting time-dependent density-functional theory for photochemical applications: Oxirane. *J. Chem. Phys.* **2007**, *127*, 164111.

[65] Gritsenko, O.; Baerends, E. J. Asymptotic correction of the exchange-correlation kernel of time-dependent density functional theory for long-range charge-transfer excitations. *J. Chem. Phys.* **2004**, *121*, 655–660.

[66] Dreuw, A.; Head-Gordon, M. Single-reference *ab initio* methods for the calculation of excited states of large molecules. *Chem. Rev.* **2005**, *105*, 4009–4037.

[67] Ryabinkin, I. G.; Ospadov, E.; Staroverov, V. N. Exact exchange-correlation potentials of singlet two-electron systems. *J. Chem. Phys.* **2017**, *147*, 164117.

[68] Nazarov, V. U.; Vignale, G. Optics of semiconductors from meta-generalized-gradient-approximation-based time-dependent density-functional theory. *Phys. Rev. Lett.* **2011**, *107*, 216402.

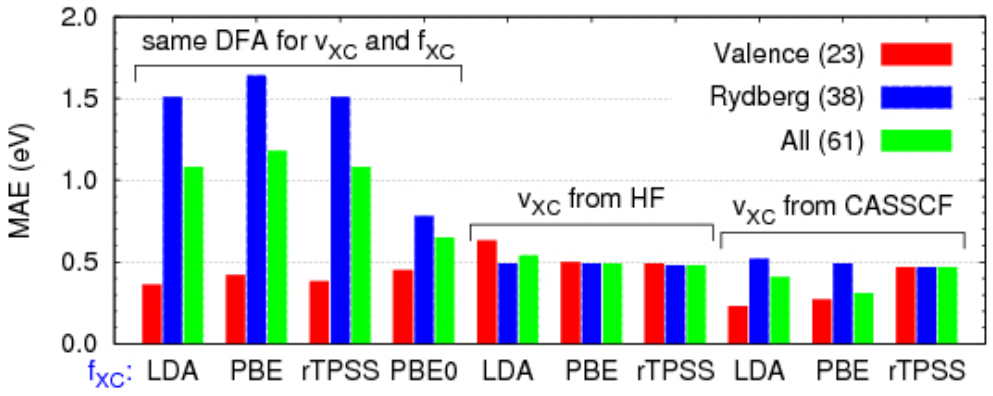

TOC graphic

45x18mm (300 x 300 DPI)